EARTH RESEARCH FROM SPACE, 2006, No 6

UDK 528.88: 551: [502.330.15] (9-929.9)

MONITORING POLLUTION OF THE OCEAN COASTAL WATER AREAS USING HIGH RESOLUTION SPACE MULTISPECTRAL IMAGERY

© 2006. V.G. Bondur*, R.N. Keeler **, S.A. Starchenkov*, N.I. Rybakova*

AEROCOSMOS Scientific Center of Aerospace Monitoring, (495) 632-16-54,

vgbondur@aerocosmos.info

***Directed Technologies, Inc. (DTI), 3601 Wilson Blvd., Suite 650 Arlington, VA 22201,*

Norris_keeler@directedtechnologies.com

The results of processing high resolution (~2…4 m) multispectral space imagery of the ocean surface, obtained for the purpose of monitoring of coastal water area pollution are presented in this paper. The image processing method based on the analysis of signal relative variability characteristics in 60÷80 nm *R, G, B* spectral bands was applied [3]. Sea truth hydrooptical AC-9 measurement results were also used during monitoring. The biooptic model for polluted waters has been created on the base of vertical profiling of absorption and scattering spectra. Analysis results both of multispectral space images and sea truth hydrooptical and hydrophysical measurements have shown their good correspondence. Hydrooptical anomalies caused by intensive submerged wastewater discharges have been detected with their geometric parameters as a result of processing of ocean multispectral images. This method can be used for the solution of various issues of monitoring of littoral ocean regions using space multispectral high resolution imagery.

INTRODUCTION

At present, one of the most important directions of the Ocean study is the study of its coastal zones. This is caused by the fact that these regions undergo intensive anthropogenic impacts, most essential of which are deep wastewater discharges into the ocean. The dynamics of different processes in coastal zone of the ocean, which was subjected to impacts of such type, is investigated insufficiently. The methods of in-situ measurements, although they possess high accuracy, are very expensive and do not make it possible to obtain the complete picture of distribution of the plumes of pollution through large spaces. Therefore the monitoring of coastal water areas using satellite methods and technologies in the present time is extremely urgent [1, 2] .

One of the perspective means of remote monitoring of environmental conditions of coastal water areas, which are undergoing intensive anthropogenic impacts, is multispectral space survey from onboard of high spatial resolution satellites [1-3]. The use of data obtained from satellites, equipped with multispectral equipment allows us the following [1-4]:

- To evaluate the quality of waters in the coastal zones and to conduct their monitoring;

- To analyze the environmental conditions of water areas;

- To investigate various dynamic processes, such as mesoscale vortices, changeability of frontal zones, propagation of river drains, etc;

- To determine variations in hydrooptical characteristics, in the first place of color and turbidity due to fluctuations of light scattering and absorption coefficients under conditions of changing concentrations of suspended and absorbing materials;

- To control biological parameters (phytoplankton conditions and bioproductivity in the ocean, etc.);

- To determine the bottom relief in the shelf zones, and also its changes under the influence of different processes, etc;

Along with the multispectral space equipment, in the present time hyperspectral sensors, which make it possible to obtain information with high spectral resolution with relatively low spatial resolution are actively used [1, 5].

The multispectral space survey with high and middle spatial resolution (under condition of synchronous sea truth measurements) allows us to determine absolute values of a number of characteristics of marine environment taking into account measurements the ocean color (power of upwelling radiation in the narrow spectral intervals) and to carry out the analysis of the time and spatial variability of these characteristics [1-3].

Now state-of-the-art satellites with multispectral equipment allow us to obtain images with very high spatial resolution (~ 2 … 4 m).

To detect optical anomalies of water environment, caused by anthropogenic impacts, the application of special methods and algorithms of satellite information processing is necessary. This work suggests the method for detection of low-contrast anomalies of water environment, caused by anthropogenic impacts, based on the characteristics of signal variability in high spatial resolution spectral bands. Based on the proposed method, the comprehensive monitoring of Mamala Bay (Hawaii) coastal water area was carried out,

as well as anomalies due to deep wastewater discharge were detected and their spatial and geometric characteristics were determined.

FUNDAMENTAL CHARACTERISTICS OF THE OBJECT OF INTEREST, SPECIAL FEATURES OF DATA ACQUISITION

For the majority of coastal water areas of the Ocean, the problem of the disposal (damping) of discharged water is very urgent. The discharged water affects substantially the environment of these regions. In the framework of this effort there were conducted studies in the Mamala Bay water area, located in the southern part of Oahu island of Hawaiian archipelago (Fig. 1) [2, 6-8]. In the same region there are located the world-known Waikiki resorts (Fig. 1).

The Sand Island Wastewater Treatment Plant (WWTP) with the capacity more than 300000 m^3/day has the deep discharge collector with a length about 3.8 km (Fig. 1) [www.hwea.org]. The impact of such a volume of the discharges waters into the water area of bay on the ecosystems in the region of recreational zone is investigated insufficiently.

Along with other satellite data, during the comprehensive monitoring of the Oahu Island coastal water area with the purpose of detecting water environment anomalies caused by such deep wastewater discharge, high spatial resolution QuickBird and IKONOS multispectral imagery were used [2].

Fig. 2 gives the exampled characteristics of the spectral transmission of surveying equipment of the QuickBird satellite in blue, green, red, close infrared, and panchromatic bands. Fig. 3 represents the exampled fragments of original space images, obtained on August 16 (imaging time 11:14:52, local) and on September 3 (imaging time 11:15: 37, local) 2004.

To verify the results of multispectral space imagery processing in the studied water area there were conducted sea truth measurements using AC-9 hydrooptical equipment and various hydrophysical equipment at the moments of time close to the moments of the space survey [2,6-8]. Spectral lines, which correspond to the centers of the AC-9 spectral bands, are given in Fig. 2. The sensor was deployed from the "Klaus Wyrtki" ship using hydraulic winch and crane with 0.4 m/s average speed of sinking at the depth near 150 m (see Fig. 4). Using AC-9 there were measured the values of absorption (k, m^{-1}) and attenuation (ε, m^{-1}) coefficients at nine wavelengths (in 412 to 715 nm spectral range) at each station (B6), which are located in the region of the diffuser. The elevation profiles for these coefficients were built according to the obtained data for each station, in which the measurements were conducted.

DATA PROCESSING PROCEDURE

To process the AC-9 information we used the method based on the Haltrin-Kopelevich linear biooptical model [9, 10], which allows us to calculate admixture concentrations (such as chlorophyll_a, dissolved organic matter, small and large particles) taking into account hydrooptical data [9-12]:

$$a(\lambda) = aw(\lambda) + Cap(\lambda) + Yay(\lambda),$$

$$b(\lambda) = bw(\lambda) + NPsbPs(\lambda) + NPlbPl(\lambda),$$

where: a (λ) and b (λ) are admixture absorption and scattering coefficients (m^{-1}); λ is the wavelength (nm); aw (λ) and bw (λ) are absorption and scattering coefficients of clean sea water (m^{-1}); C - total chlorophyll_a concentration (mg/m^3); Y is dissolved organic matter concentration (arbitrary units); ap (λ) is a specific absorption coefficient of the basic phytoplankton mixture (18 kinds) – (m^2/mg); ay (λ) is the specific absorption coefficient of the dissolved organic matter (m^{-1}); N is the number of admixtures; Ps, Pl are the concentrations of small and large particles (g/m^3); bPs (λ) is the specific scattering coefficient of small particles (m^2/g); bPl (λ) is the specific scattering coefficient of large particles (m^2/g);

For all stations, at which there were conducted the AC-9 measurements using vertical profiles of absorption and scattering coefficient spectra there were evaluated the profiles of basic admixture concentrations using this technique.

High spatial resolution multispectral space image processing was conducted using the characteristics of relative signal variability in red (R), green (G), and blue (B) spectral bands with widths of 60-80 nm [3].

The processing technique consisted in the use of the following base procedures [1, 3, 13]:

- Synthesizing colored image from separate spectral bands (RGB-synthesis);

- Interpreting images to detect cloud cover, ships and traces of their motion, land and sea surface uncovered by clouds;

- Selecting the fragments of the full image frame in the region of interest for further processing;

- Applying filtration procedures;

- Applying decorrelation stretch procedure to eliminate the correlation of spectral bands;

- Applying the procedures of parametric and nonparametric classification;

- Applying the procedures of integration of classes;

- Applying the colorcoding procedures.

To correct image brightness distortions, caused by heterogeneous sensitivity of QuickBird CCD-camera, the following additional special procedures were used:

- Division of an image into fragments on the basis of the analysis of the pre-processing results;

- Elimination of bright transverse trend in the limits of each strip (fragment);

- Mutual leveling off brightness over the strips on the basis of statistical parameters.

Using this technique, the processing of multispectral imagery obtained from onboard of the high resolution satellites was carried out. For the verification the comparison of the obtained results with the results of processing sea truth data was accomplished and conclusions about the correctness of satellite data processing were done.

MULTISPECTRAL SPACE IMAGERY AND SEA TRUTH DATA PROCESSING RESULTS

IKONOS and QuickBird multispectral space imagery were processed during the monitoring.

Fig. 5 shows the processing results for multispectral images, obtained from the QuickBird satellite on August 16, 2004. As it is evident from the analysis of the given figure, the hydrooptical anomaly of water environment, detected using the applied technique, has well distinguishable boundaries what made it possible to conduct its outlining and to determine spatial and geometric characteristics. As we can see in Figure 5, the hydrooptical anomaly is elongated from the east to the west and has the following dimensions: ~3.5 km from the north to the south, and ~12 km from the east to the west. The greatest intensity anomaly reaches after 2 - 2.5 km to the southeast from the end of the diffuser. The fact that the anomaly is attributed to the discharge diffuser testifies its anthropogenic origin.

The results of processing the multispectral images, obtained from the same satellite on September 3, 2004, are given in Fig. 5b. As it follows from the analysis of this figure, on the surface and in the near-surface layer of ocean as in the previous case the anomaly was detected which was caused by deep wastewater discharge. Analysis of Fig. 5 b shows that the anomaly has relatively clear boundaries of "mitten-like" shape [1, 2, 7]. The dimensions of southwestern lobe from the end of Sand Island Outfall were about 4 km, and southeastern one were about 3 km.

Thus, the use of the proposed technique of high spatial resolution multispectral space image processing have allowed us to detect the anomalies, caused by the deep wastewater discharge into the water area of Mamala bay, and to determine their spatial characteristics. In this case one should note that these anomalies were not detected in the initial images before the processing.

To carry out sea truth measurements, the following types of equipment were used:

- AC-9 for hydrooptical measurements;

- MSS (Microstructure Sensors) for microstructural measurements;

- CTD (Conductivity, Temperature, Depth) for measurements of hydrophysical parameters;

- ADP (Acoustic Doppler Profiler) for measurements of current velocity;

- Drifters (Drogues) for analysis of currents;

- Secchi disk for the estimation of visibility depth;

- Equipment for ocean level measurements (Honolulu station);

The results of sea truth data processing are given in Figs. 6-9.

Fig. 6 presents the points and routes of the measurements of various parameters using the given equipment (see legend), carried out on August 16, 2004. The results, obtained during the processing of measurement results by various sensors that day, are given in Fig. 6 (b- d): tidal mode (NOAA data) – b; bathymetrical distribution of coefficient of backscattering (MSS equipment, see legend) – c; bathymetrical distribution of salinity (d) and temperature (e) (CTD equipment, B6-1 – B6-4 measuring points); wind direction and speed, measured by ship anemometers at the moment of survey, wind speed is reduced to the standard horizon 10 m (a, see legend); average current velocities at the horizons of 30 m (D5 drifter, see legend), 50 m (D2 drifter, see legend), 90 m (D4 drifter, see legend).

Fig. 7 gives the two-dimensional distributions of absorption (b), scattering (c), and attenuation (d) coefficients, obtained by AC-9 at B6-1 – B6-4 points, and also the biological characteristics calculated using them (based on the Haltrin-Kopelevich biooptical model): the concentration of chlorophyll_a (e), the concentration of dissolved organic matter (f) and the large particles (g). Also, Fig. 7 (b-g) shows the results of visibility depth measurements, carried out a Secchi disk.

Similar sea truth measurements were carried out on September 3, 2004 (Figs. 8, 9). During that day, the multispectral space survey was supported with AC-9 measurements at all B6-1 – B6-7 points. Furthermore, unlike the experiment carried out on August 16, 2004, there were performed the measurements using ADP at ADP-2 and ADP-3 points (see legend). Fig. 8 presents the points and routes of sea truth measurements using various sensors (see legend), carried out on September 3, 2004. The processing results are shown in Fig. 8 b-g: tidal mode (NOAA data) – b; bathymetrical distribution of backscattering coefficient (MSS, see legend) – c; perspective and vector flow charts at the horizons of 29.5 m and 49.5 m at ADP-2 – d, e; bathymetrical distribution of temperature (f) and salinity (g) (CTD, B6-1 – B6-4 measuring points); wind direction and speed, measured by ship anemometers at the moment of the survey, wind speed is reduced to the standard horizon of 10 m (a, see legend); average current velocities at the horizons of 30 m (D5 drifter, see legend), 50 m (D2 drifter, see legend), 90 m (D4 drifter,

see legend).

Fig. 9 similar to Fig. 7 represents the two-dimensional distributions of absorption (b), scattering (c), and attenuation (d), obtained by AC-9 at B6-1 – B6-7, and also the and also the biological characteristics calculated using them: chlorophyll_a concentration (e), dissolved organic matter concentration (f) and concentration of large particles (g). As for 16 August 2004 Fig. 9 (b- g) gives results of Secchi disk measurements.

Thus, as a result of space imagery and sea truth measurement processing there was formed the set of data, that allow us with the high degree of accuracy and reliability to estimate the impact of pollutants on the water area of interest.

THE ANALYSIS OF THE OBTAINED RESULTS

Hydrooptical heterogeneities of the near-surface layer of ocean, caused by the deep wastewater discharge from the Sand Island WWTP into the Mamala Bay water area detected as a result of multispectral imagery processing, can be discovered also on the basis of sea truth hydrooptical data, obtained by the AC-9 instrument [www.wetlabs.com]. Moreover, in the case of the accurate interpretation of space images, the results obtained by remote means should coincide with the data of sea truth measurements.

The QuickBird multispectral images having high spatial resolution, make it possible to obtain precise information about the attitude of hydrooptical anomalies [3]. Such data on vertical hydrooptical characteristics were obtained using AC-9. We used the following technique of comparison:

- The boundary of anomaly, obtained on the basis of the outlining of the results of the detection of the anomalies, caused by the deep wastewater discharge, using multispectral images, with the aid of GIS means was combined with the broken line, formed as a result of sequential combining of the points (B6-1 – B6-7), in which hydro-optical AC-9 measurements from the ship “Klaus Wyrtki" were done.

- The obtained broken line B6-1 – B6-7 was combined with the two-dimensional images of bathymetrical distribution of absorption, scattering, and attenuation coefficients, calculated according to AC-9 data at the wavelength of 0.488 m;

- The combination of this line was performed with the calculation results for such parameters as concentrations of chlorophyll, dissolved organic matter, content of large suspended particles, calculated according to hydrooptical data, and also with the results, obtained using a Secchi disk;

- The coincidence of the anomaly boundary detected according to the space images and according to AC-9 data was evaluated. Then, taking into account the sea truth hydrophysical data processing results, the conclusions about the correctness of the anomaly detection using satellite data were made;

To compare with satellite imagery processing results, there were used absorption and attenuation coefficients, obtained by AC-9 at the wavelength of λ=0.488 m. This choice was stipulated, in the first place, by the fact that for this wavelength the absorption of sunlight by waters of the Pacific Ocean in the region of Hawaiian islands was close to the minimum [14, 15]. Furthermore, the AC-9 spectral band λ=0.488 m coincided with the center of the blue band of the QuickBird equipment. This is clear from Fig. 2.

Figs. 6 and 7 show the exampled results of the comparison of space and sea truth hydrooptical and hydrophysical data, obtained on August 16, 2004.

Since on August 16, 2004 AC-9 measurements were conducted only at B6-1, B6-2, B6-3, and B6-4 stations (see Fig. 7), the evaluation of coincidence of the anomaly boundaries, detected using multispectral images, with sea truth hydrooptical data was carried out only for the eastern zone of anomaly.

Analysis of Figs. 6 and 7 testifies good agreement of the eastern boundary of anomaly, detected using the space images, and the region of the increased values of the coefficients of scattering, absorption, and attenuation, located in layer of jump on the depth near 50 m, detected using AC-9 data. Combination of anomaly boundaries detected using multispectral satellite imagery and sea truth hydrooptical data on the horizontal plane gives the discrepancy of 200-300 m, which is completely acceptable.

Thus, it is possible to assert that the region of the increased values of hydrooptical characteristics mentioned above is caused by the deep wastewater discharge, which is confirmed also with the analysis of such parameters as the concentration of chlorophyll_a, dissolved organic matter and large particles, whose maximum values were observed in the anomalous region described above (Fig. 7).

Measurements by Secchi disk at the B6-3 station showed that the maximum visibility at this point was on the average 45.5 m, while at the stations B6-7 it was 50.47 m. Obviously, this is explained by the fact that the reason for decrease of maximum visibility at B6-3 is the presence of the concentrations of different substances (organic matter, suspension, etc), which are contained in the effluents, in the layer of jump (Fig. 7). The value of maximum Secchi visibility very well coincides with the characteristics, calculated according to AC-9 measurement data i.e. concentrations of chlorophyll_a, the dissolved organic matter, and large particles (Fig. 7) – upper boundary of the zone of their increased concentrations in the layer of jump coincides with the value, obtained by the disk at B6-3. Thus, Secchi data analysis also confirms the correctness of the detected anomaly in the multispectral images.

Directions of drifter moving at various depths (D2 (50 m), D4 (90 m), and D5 (30 m) in Fig. 6 correspond to the flood phase (Fig. 6b) and stipulate the orientation and extent of the eastern part of the hydrooptical anomaly.

The presence of the sufficiently extensive western part of the anomaly can be explained by the fact that this anomaly was formed earlier, at the ebb phase.

MSS data, particularly backscattering (Fig. 6c), demonstrate the presence of a region with the increased values of scattering in the direction to the south from the diffuser up to the distance of ~1 km. The depth of this region is about 50 m, what coincides with AC-9 data.

According to the data about the depth of the jet floating-up at the moment of QuickBird imaging on August 16, 2004 (11:14), obtained according to the results of numerical simulation, the depth of the jet floating-up was ~54 m [16]. As it is evident from Fig. 7 (b-g), very good agreement of model calculations and AC-9 data is evident, and the depth of the jet floating-up correspond to the region of the maximum values of scattering, absorption, and attenuation coefficients, and also to the calculated values of concentrations of chlorophyll_a, dissolved organic matter, and large particles.

The results of the joint analysis of multispectral space and in-situ AC-9 data, obtained on September 3, 2004, are given in Figs. 8 and 9.

The processing results for multispectral satellite images taken on that day, just as for August 16, 2004 coincide well with the results of sea truth measurements. As the analysis of the processing results have shown, high degree of the agreement both of the eastern and western boundaries of anomaly, detected using satellite multispectral images, with the anomaly, detected using two-dimensional depth distributions of hydrooptical parameters (scattering and attenuation coefficients), registered by AC-9 was observed (Fig. 9).

The results obtained using Secchi disks have shown that at B6-3 and B6-5 stations (near the diffuser) maximum visibility was about 48-51 m, while at B6-7 station (far from the diffuser) the depth was 55.5 m. It is obvious that the reason for decrease of maximum visibility at B6-3 and B6-5 stations was the increased concentration of different substances (organic matter, suspension, etc) contained in the effluents, near the layer of jump (Fig. 9). The value of maximum Secchi visibility also coincides very well with the characteristics, calculated according to AC-9 measurement data – chlorophyll_a, the dissolved organic matter, and large particles (Fig. 9 e, f, g) – upper boundary of the zone of their increased concentrations coincides with the values, obtained using the disk at B6-3 and B6-5 stations.

The increased values of primary hydrooptical characteristics and calculated admixture concentrations, as well as relatively low values of Secchi visibility, in the region of B6-1 station can be caused by the influence of the Ala Wai drainage (see Figs. 7 and 9).

According to MSS data, obtained on September 3, 2004, the depth of the anomaly, caused by the deep wastewater discharge, was approximately 60 m. This coincides very well with AC-9 data (~58 m).

Directions of drifter moving at various depths (D2 (50 m), D4 (90 m), and D5 (30 m) in Fig. 9a correspond to the flood phase (Fig. 6b) and correlate very well with the orientation of the corrected lobe of the eastern part of the anomaly detected using the multispectral satellite image.

The effects of current direction changes caused by tidal phenomena, are evidently demonstrated by the data ADP2, obtained at the horizons of 29.5 m (Fig. 8 d), 49.5 m (Fig. 8 e). In the time interval from 5 to 12 hours LT on September 3, 2004 the transfer direction at the horizon of 29.5 m changes by 180 degrees (from ~300° to ~120°) after the change of the flood phase, at that time at the horizon of 49.5 m (near the layer of jump) the direction of transfer does not change. Thus, in the layer of jump in the time interval from 5 to 12 hours the transfer remained in the direction ~120°, that also caused the appearance of an eastern lobe of the anomaly, most vividly detected according to the results of hydrooptical measurements at the depths of ~ 50… 70 m.

Quite intensive manifestation of thermohaline stratification processes in the region of deep drain was revealed according to CTD data, obtained by "Klaus Wyrtki"(Fig. 8 f, g). The region, where these effects appear most intensively, coincides with the region of the maximum values of the parameters, determined according to AC-9 data (see Figs. 8, 9). This agree well with the physical ideas and the results of simulation.

Model calculations of the jet floating-up depth at the moment of QuickBird imaging on September 3, 2004 (11:16) have shown that this parameter was equal to ~53 m [16]. Comparison with the two-dimensional distributions of the parameters, obtained according to AC-9 data (Fig. 9, b-g) has shown that there was good agreement of model calculations of the jet floating-up depth and the region of maximum values, the measured coefficients of scattering and attenuation, and also calculated values of the coefficients of absorption, concentrations of chlorophyll_a, dissolved organic matter, and large particles. It has been shown that the jet floating-up depth corresponded to upper boundary of the maximum values of the parameters indicated.

Such close coincidence of AC-9 data (Fig. 9) and the results, obtained using high spatial resolution multispectral satellite images, make it possible to draw the unambiguous conclusion that the detected anomaly is caused by the deep drain from the Sand Island.

During the comprehensive analysis of satellite and sea truth data, the information on one more source of anthropogenic influence on the Mamala Bay and Waikiki resort which is the Ala Wai drainage, obtained for the first time in [3] have been confirmed. The impact of this source became apparent during the analysis of AC-9 measurement data. Thus, in Fig. 9 in the mouth region an increase in the values of such parameters as the concentration of chlorophyll (Fig. 9 e) and concentration of dissolved organic matter (Fig.9 f) are observed, what is caused by discharge out of the

drainage.

Thus, the comprehensive analysis of the obtained information have allowed us to unambiguously interpret the results of processing the multispectral space images, obtained during the monitoring of anthropogenic impacts on the water environment, caused by deep wastewater discharges from drainages.

CONCLUSION

This paper presents the results of the studies, carried out using multispectral satellite imagery of high spatial resolution, as well as hydrooptical and hydrophysical data, obtained during the monitoring of coastal water areas, subjected to anthropogenic influences.

It has been shown that the capabilities of multispectral space equipment of high spatial resolution (~2 … 4 m) and the used procedure of working make it possible to investigate the small-scale changeability of ocean over the considerable areas within the layer of sea surface brightness forming.

The comprehensive analysis of the results of processing high spatial resolution multispectral space images, and also hydrooptical sea truth data have shown that dimensions and directions of propagation of the anomalies of the hydrooptical characteristics, detected using multispectral imagery, almost coincide with spatial distributions of primary hydrooptical parameter fields and the derived characteristics (concentrations of chlorophyll, dissolved organic matter, large and small particles and other), obtained by AC-9.

Comparison and analysis of satellite and sea truth (hydrooptical and hydrophysical) data have allowed us to conduct the validation of the results of high spatial resolution multispectral satellite image processing and to confirm their high efficiency during monitoring of coastal water areas.

REFERENCES

1. *Bondur V.G.* Aerospace methods in modern oceanology/ In “New ideas in oceanology”. Moscow: Nauka, Vol. 1: Physics. Chemistry. Biology. 2004. p. 55 – 117.

2. *Bondur V.G.* Complex Satellite Monitoring of Coastal Water Areas. 31st International Symposium on Remote Sensing of Environment, June 20-24, 2005, Saint Petersburg, Russian Federation.

3. *Bondur V.G., Zubkov E.V.* Detection of small-scale inhomogeneities of optical characteristics of ocean upper layer by high resolution multispectral satellite imagery. Part I. Effects of drainage runoffs into coastal water areas// Issledovanie Zemli iz Cosmosa, 2005, No 4, pp. 54-61.

4. *Kopelevich O.V., Burenkov V.I, et al.* Optical methods in oceanology and marine geology // in the book. “New ideas in oceanology. Physics. Chemistry. Biology ". Moscow: Nauka. 2004. Vol. 1. Pp. 55-117.

5. *Grace Chang, Kevin Mahoney, Amanda Briggs, et al.* The new age of hyperspectral of oceanography // Oceanography, 2004, pp. 22-29.

6. *Keeler R., Bondur V. Vithanage D.* Sea truth measurements for remote sensing of littoral water // Sea Technology, April, 2004, p. 53-58.

7. *Keeler R., Bondur V.G, Gibson C.* Optical satellite imagery detection of internal wave effects from a submerged turbulent outfall in the stratified ocean //Geophisical Research Letters, Vol. 32, L12610, doi:10.1029/2005GL022390, 2005.

8. *Bondur V.G., Tsidilina M.* “Features of Formation of Remote Sensing and Sea truth Databases for The Monitoring of Anthropogenic Impact on Ecosystems of Coastal Water Areas.” 31st International Symposium on Remote Sensing of Environment. ISRSE, 2006. 192-195.

9. *Kopelevich O. V.* Small parameter model of optical properties of sea water. Chapter 8 // *Ocean Optics, Vol. 1: Physical Ocean Optics*, (A. S. Monin, Ed., Nauka Publishers, Moscow, 1983).

10. *Haltrin V.I. and Kattawar G.W.* Self-consistent solutions to the equation of transfer with elastic and inelastic scattering in oceanic optics: The I. Model // *Applied Optics*, 1993. Vol. 32. No. 27. P. 5356-5367.

11. *Pope R.M. and Fry E.S.*. Absorption spectrum (380 – 700 nm) of pure water, II. Integrating cavity measurements // *Applied Optics*, 1997. Vol. 36. P. 8710 – 8723.

12. *Buiteveld H.J., et al.* The optical properties of pure of water // *Ocean Optics XIII, SPIE 2258*, 1994, pp. 174 – 183.

13. *Bondur V.G., Starchenkov S.A.* Methods and software for aerospace imagery processing and classification// Izvestia Vuzov. Geodesy and aerophotoimaging, 2001, № 3, pp. 118-146.

14. *Erlov N.G.* Marine optics //Leningrad: Gidrometeoizdat, 1980. 249 p.

15. *Ivanov A.P.* Physical bases of hydrooptics // Minsk, “Nauka I Technika ", 1975, 504 p.

16. *Bondur V.G., Grebenyuk Yu.V., Zhurbas V.M.* Mathematical simulation of turbulent jets of deep drains into the coastal water areas // Oceanology, 2006, No 6.

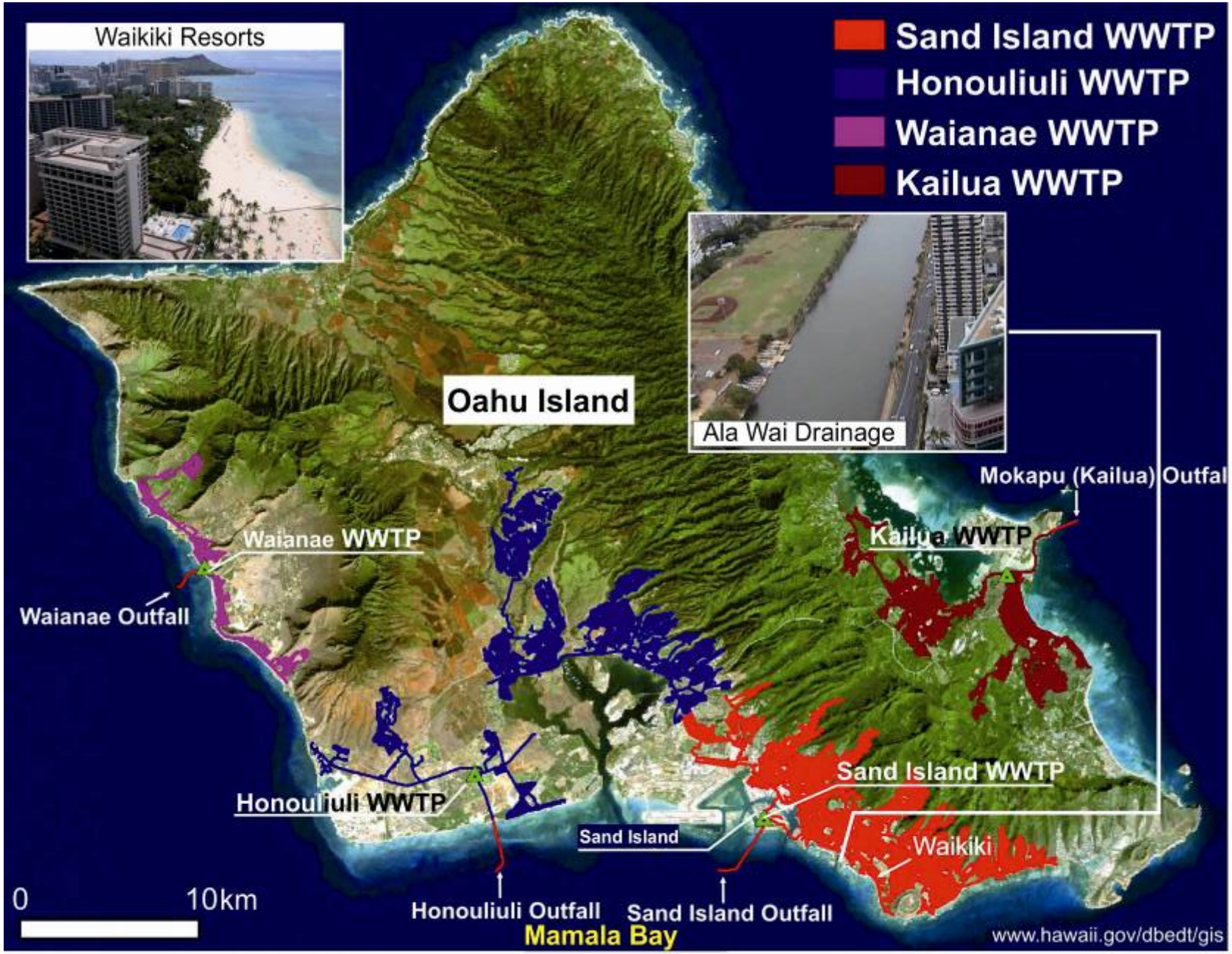

Fig. 1. Locations of wastewater treatment plants (Oahu Island) having underwater outfalls, and their service ranges

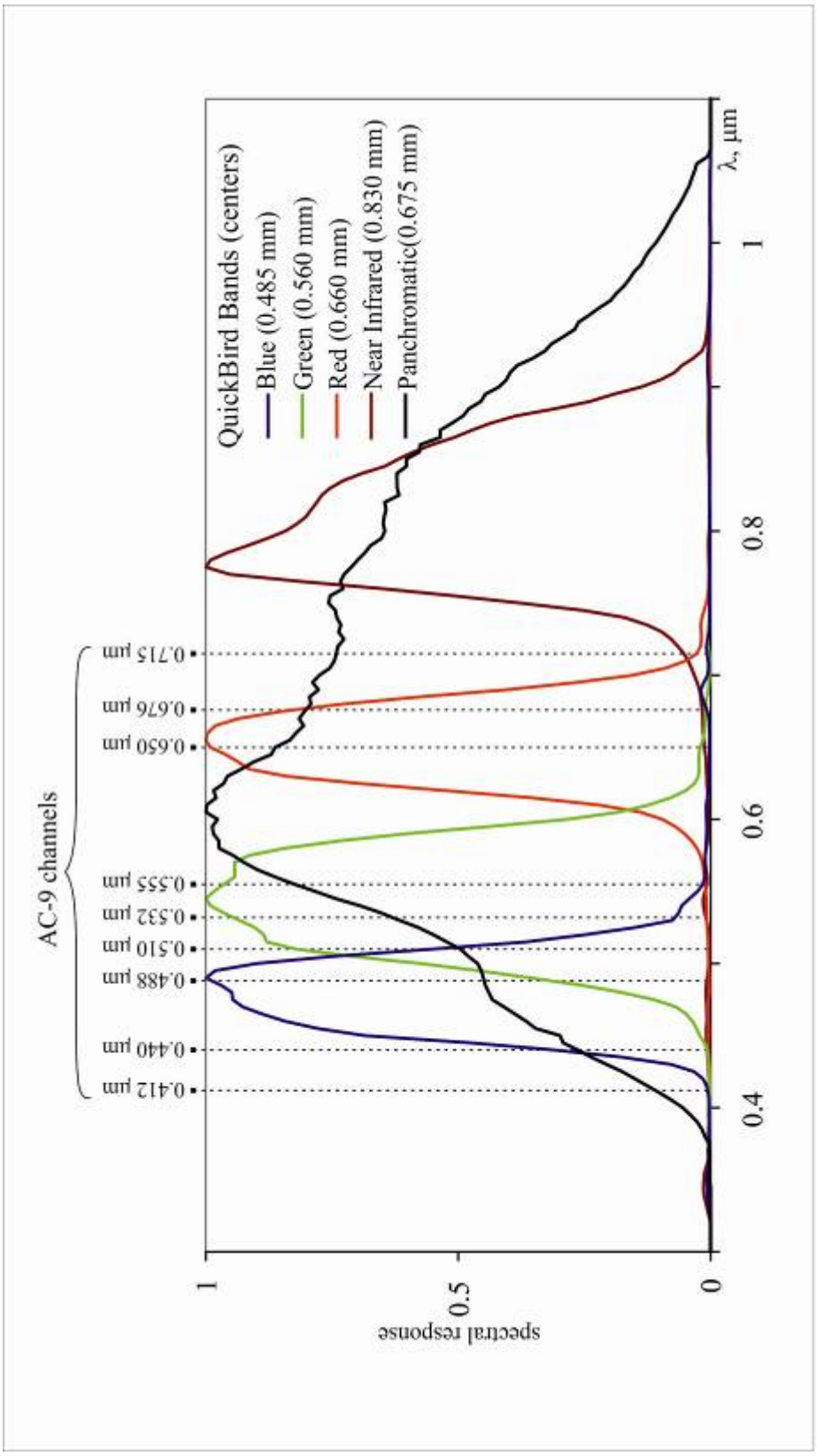

Fig. 2. Spectral characteristics of QuickBird instrument bands (www.digitalglobe.com) and AC-9 bands (www.wetlabs.com) for sea truth hydrooptical measurements

Fig. 3. QuickBird initial images obtained on August 16 (a) and on September 3 (b) 2004

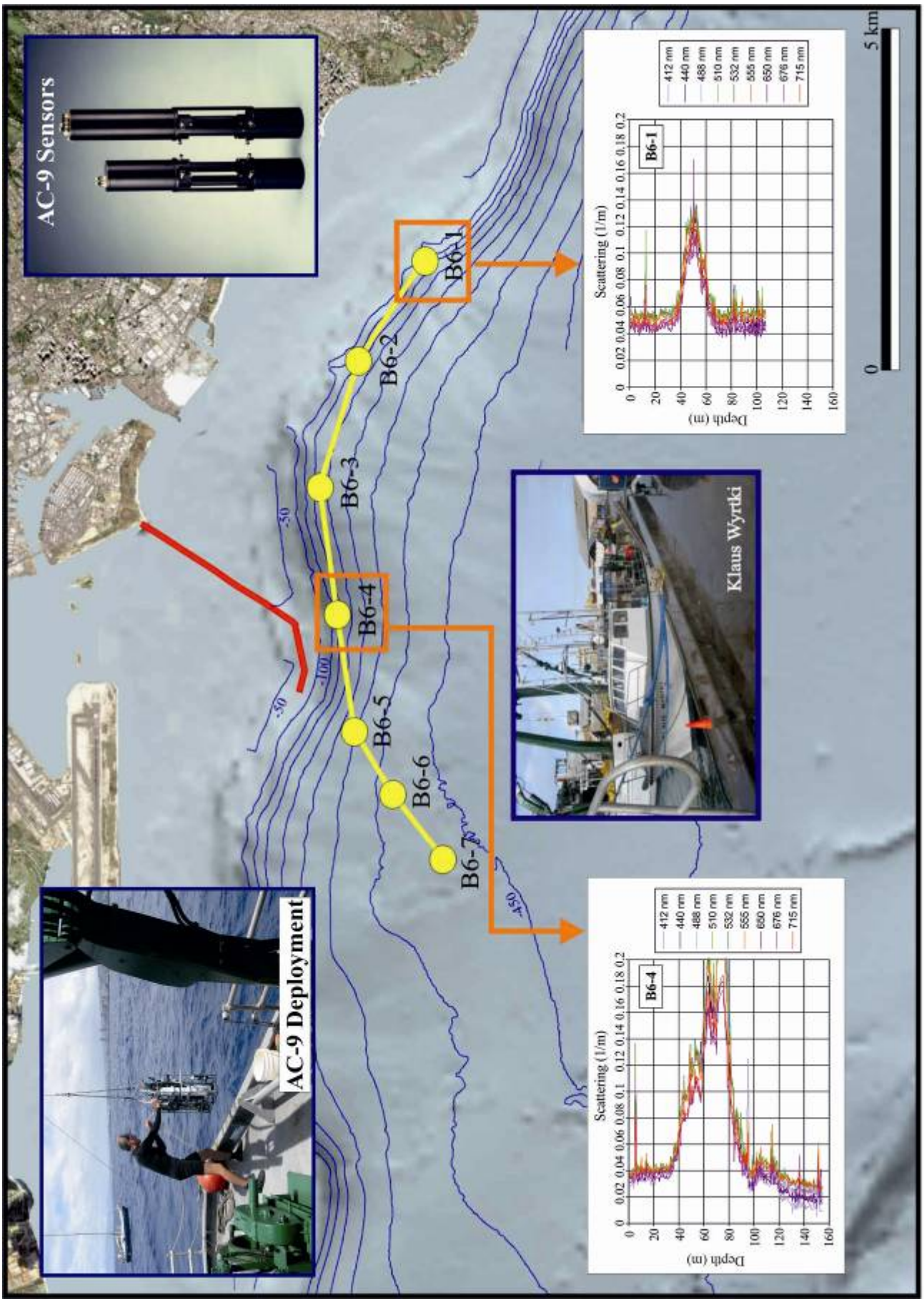

Fig.4. Measuring hydrooptical parameters using AC-9 in the Mamala Bay water area

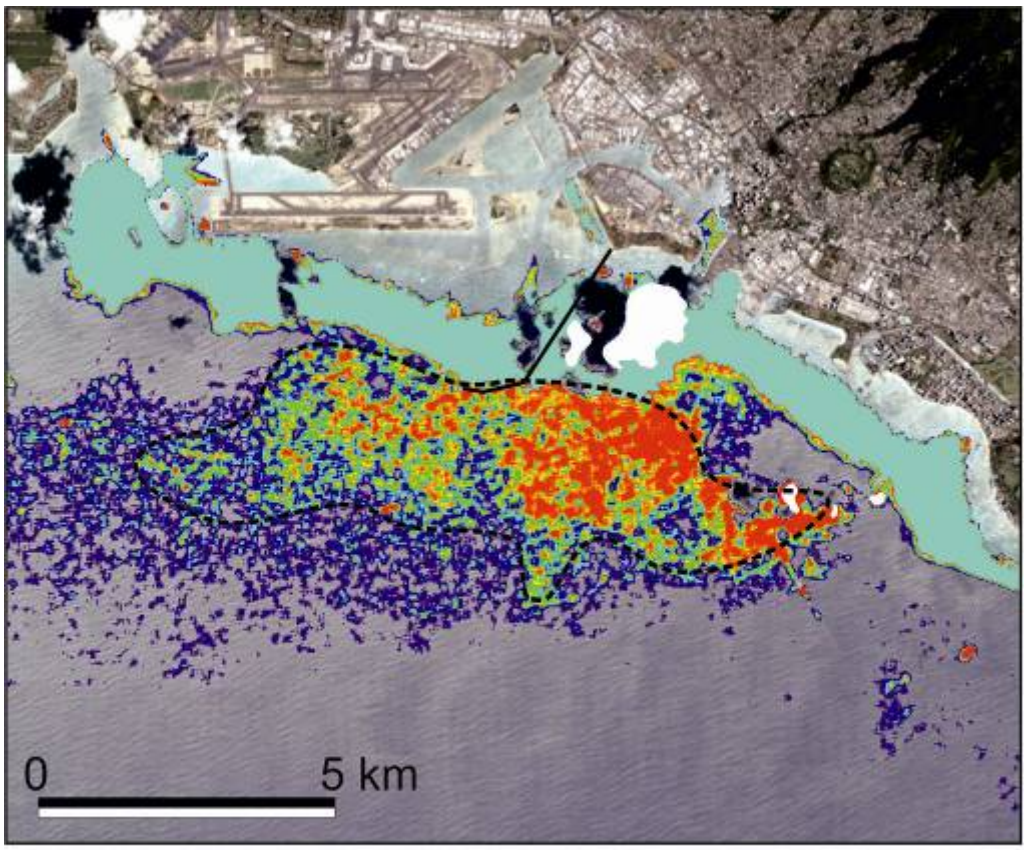

a

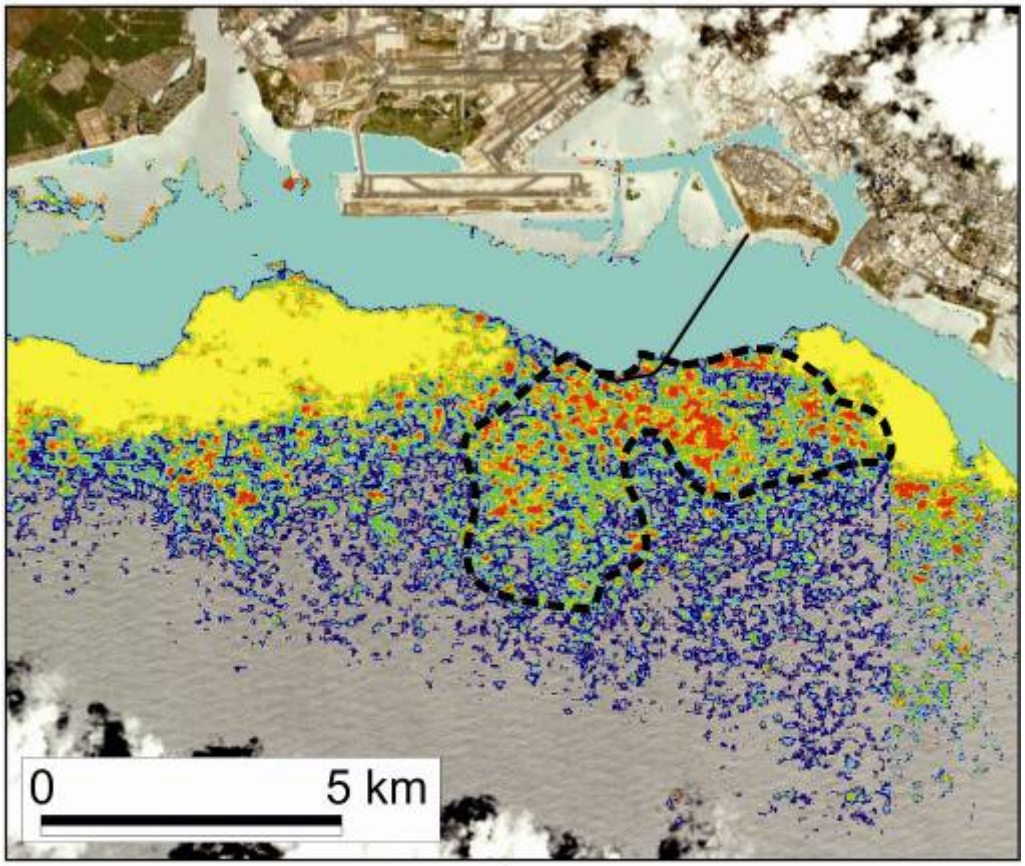

b

Fig. 5. Detecting and outlining an optical anomaly according to the results of QuickBird imagery processing (16 August (a) and September 3 (b) 2004)

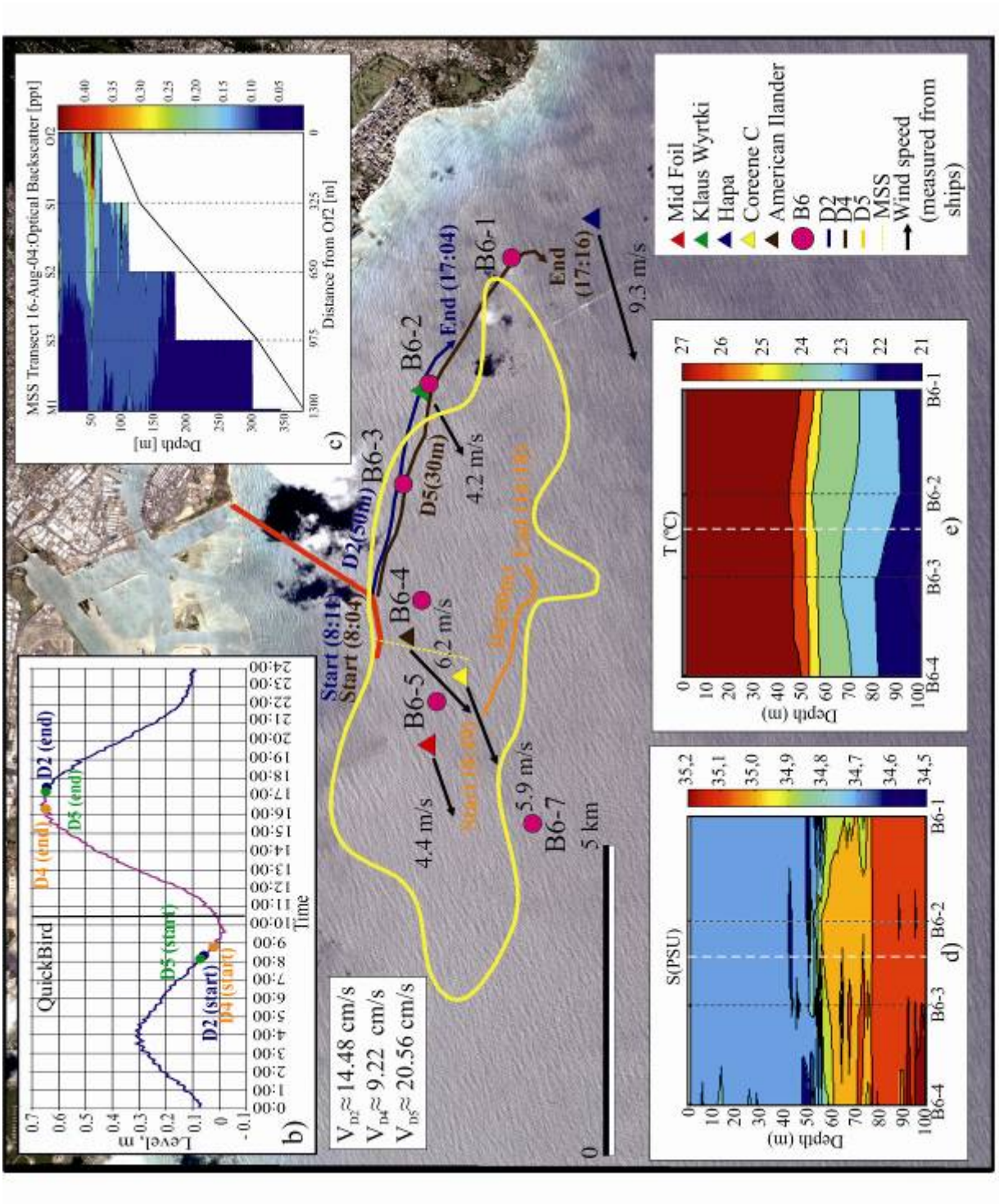

Fig. 6. The results of comprehensive comparison of the anomaly detected using QuickBird data obtained on August 16, 2004 with the data obtained using various sensors: a – the schematics of the comprehensive study; b – tidal mode; c – MSS backscattering; d – 2D salinity profile based on CTD data for B6-1 – B6-4 stations; e – 2D temperature profile based on CTD data for B6-1 – B6-4 stations

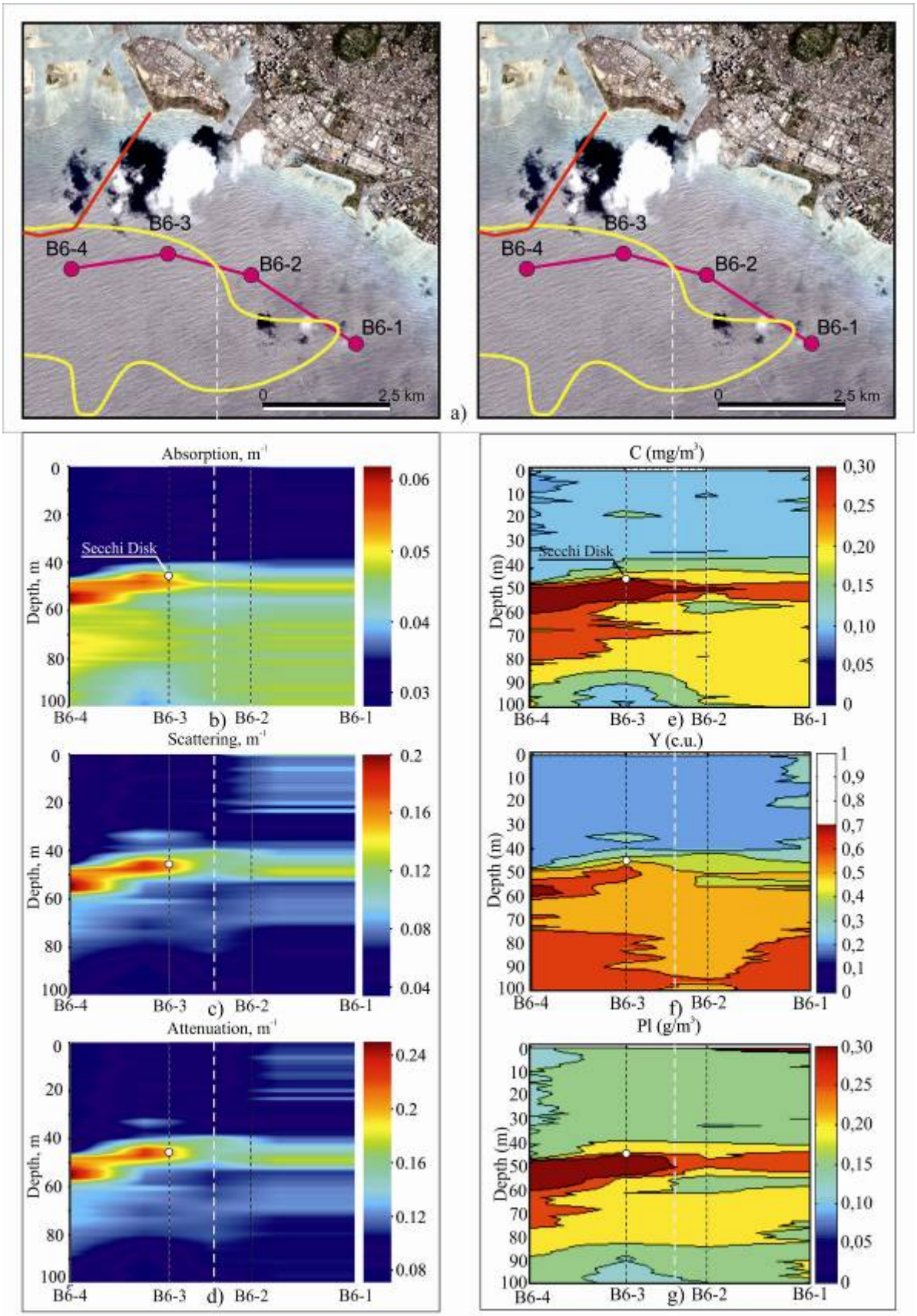

Fig. 7. The results of comparison of the anomaly detected using QuickBird data obtained on August 16, 2004 (a) with hydrooptical data: 2D cross-sections of absorption (b), scattering (c), and attenuation (d) coefficients at 0.488 мм; concentrations of chlorophyll_a (e), dissolved organic matter (f), and large particles (g), built on the base of AC-9 measurement data; Secchi maximum visibility (b-g)

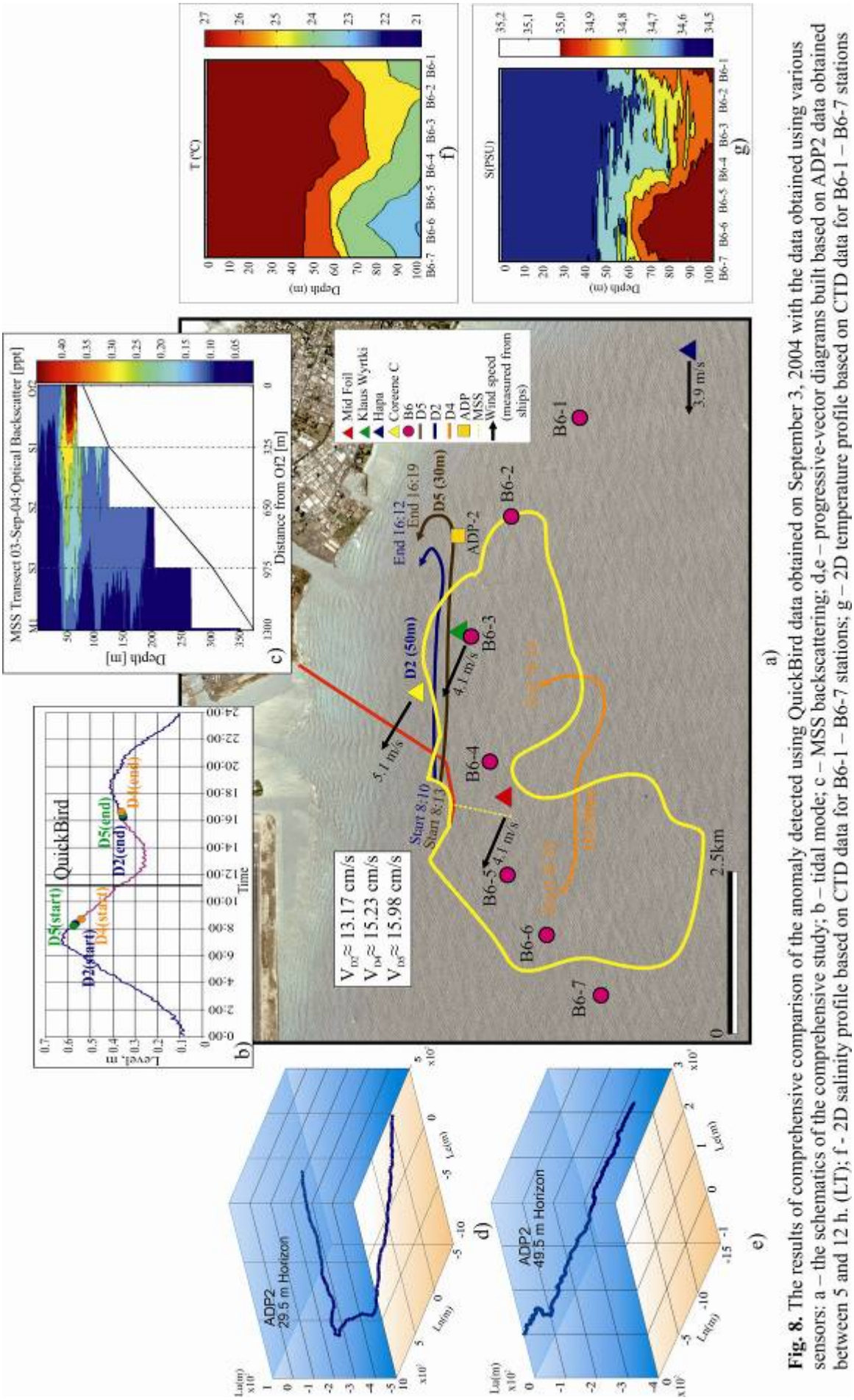

Fig. 8. The results of comprehensive comparison of the anomaly detected using QuickBird data obtained on September 3, 2004 with the data obtained using various sensors: a – the schematics of the comprehensive study; b – tidal mode; c – MSS backscattering; d,e – progressive-vector diagrams built based on ADP2 data obtained between 5 and 12 h. (LT); f - 2D salinity profile based on CTD data for B6-1 – B6-7 stations; g – 2D temperature profile based on CTD data for B6-1 – B6-7 stations

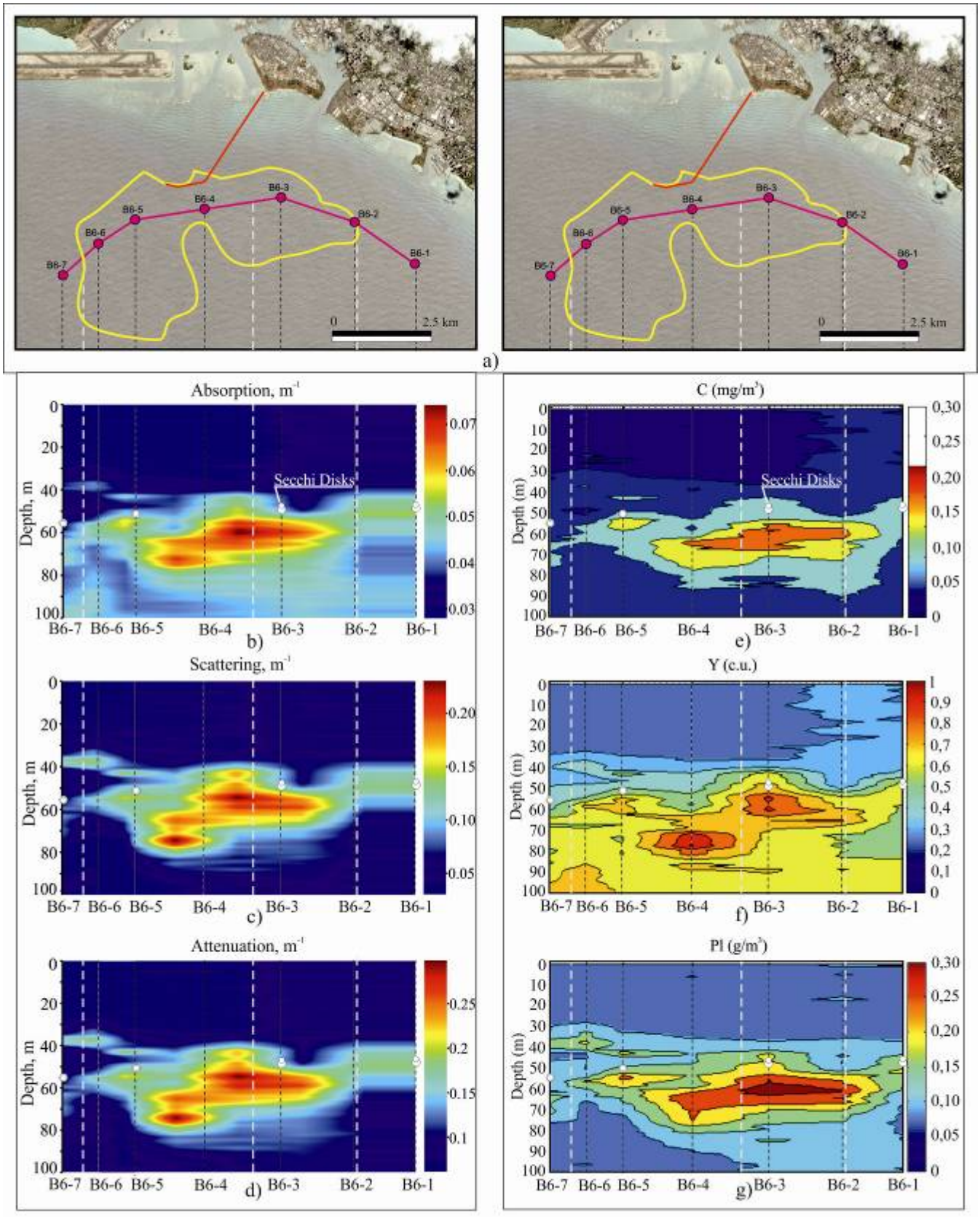

Fig. 9. The results of comparison of the anomaly detected using QuickBird data obtained on September 3, 2004 (a) with hydrooptical data: 2D cross-sections of absorption (b), scattering (c), and attenuation (d) coefficients at 0.488 мм; concentrations of chlorophyll_a (e), dissolved organic matter (f), and large particles (g), built on the base of AC-9 measurement data; Secchi maximum visibility (b-g)